Article ID: 1000-7032(2015)02-0249-07

Two-photon Absorption in ZnO/ZnS Core-shell Quantum Dots

LIU Shu-yu[1], ZHONG Mian-zeng[2], MENG Xiu-qing[2], LI Jing-bo[2,3], WANG Yuan-qian[1], XIAO Si[1], HE Jun[1*]

(1. *Hunan Key Laboratory for Super-microstructure and Ultrafast Process, School of Physics and Electronics, Central South University, Changsha* 410083, *China*;
2. *Research Center for Light Emitting Diodes (LED), Zhejiang Normal University, Jinhua* 321004, *China*;
3. *State Key Laboratory of Superlattices and Microstructures, Institute of Semiconductors, Chinese Academy of Sciences, Beijing* 100083, *China*)
* *Corresponding Author, E-mail: junhe@csu.edu.cn*

Abstract: We report a large two-photon absorption (TPA) in ZnO/ZnS and ZnO/ZnS/Ag core/shell quantum dots (QDs). Z-scan and pump-probe techniques with femtosecond laser pulses were employed to characterized the quantum dots. The intrinsic TPA coefficients of ZnO-based core/shell QDs are enhanced with nearly three orders of magnitude compared to that of ZnO bulk counterpart, which is attributable to quantum confinement effect. The TPA cross-section of ZnO-based nanocomposites is determined to be $\sim 4.3\times10^{-44}$ cm^4 · s · photon^{-1} at the wavelength of 660 nm. This value is at least two orders of magnitude greater than that of ZnS, ZnSe, and CdS QDs. Due to the local field effect, the nonlinear absorption in ZnO/ZnS core/shell QDs is improved as beaded with Ag nano-dots.

Key words: two-photon absorption; ZnO/ZnS core/shell quantum dots; Z-scan technique
CLC number: O433.1 **Document code**: A **DOI**: 10.3788/fgxb20153602.0249

ZnO/ZnS 核-壳量子点的双光子吸收效应

刘姝妤[1], 钟绵增[2], 孟秀清[2], 李京波[2,3], 王沅倩[1], 肖 思[1], 何 军[1*]

(1. 中南大学物理与电子学院 超微结构与超快过程湖南省重点实验室, 湖南 长沙 410083;
2. 浙江师范大学 LED 芯片研发中心, 浙江 金华 321004;
3. 中国科学院半导体研究所 超晶格与微结构国家重点实验室, 北京 100083)

摘要: 利用飞秒激光 Z-扫描与泵浦-探测技术,研究了室温下 ZnO/ZnS 与 ZnO/ZnS/Ag 核-壳胶体量子点的双光子吸收效应。研究发现:ZnO 基核-壳量子点的本征双光子吸收系数比 ZnO 体材料增大了 3 个数量级;测量得到的 660 nm 处的 ZnO/ZnS 核-壳量子点双光子吸收截面约为 4.3×10^{-44} cm^4 · s · photon^{-1},比相应的 ZnS、ZnSe 及 CdS 量子点大 2 个数量级;当 ZnO/ZnS 核-壳量子点镶嵌了银纳米点时,非线性吸收有所增强。ZnO 基复合纳米结构的双光子吸收增强可归因于量子限域与局域场效应。

关 键 词: 双光子吸收; ZnO/ZnS 核-壳量子点; Z-扫描技术

收稿日期: 2014-05-23; **修订日期**: 2014-07-14
基金项目: 国家自然科学基金(61222406,11174371,11104250); 湖南省自然科学基金(12JJ1001); 教育部博士学科点专项科研基金(20110162120072); 教育部新世纪优秀人才支持计划(NCET-11-0512)资助项目

1 Introduction

In the past decade, there has been great interest in the nonlinear optical and photoluminescence (PL) properties of nanocrystals[1-10]. Two-photon absorption (TPA) properties of quantum dots have received widespread attention, which may have technological applications such as bio-imaging, optical-switching devices, quantum-dot lasers, or light emitters[11]. While multi-photon absorption properties in ZnO and ZnS quantum dots (QDs) have been observed by Z-scan technique and pump-probe measurements[12-16], there is little research on ZnO-based core/shell nanocomposite quantum dots[17]. Compared to pure ZnO and ZnS QDs, ZnO-based core/shell structures usually have an improvement in physical and chemical properties for electronics, magnetism, optics, catalysis, mechanics, and others[18-19]. Although theoretical and experimental TPA research has made great progress, there still has the limitation of existing nonlinear optical materials and further studies are needed[2]. In this paper, we report an investigation on TPA in ZnO/ZnS and ZnO/ZnS/Ag core/shell QDs, which was determined by femtosecond Z-scan technique and pump-probe measurements at the non-resonant wavelength of 660 nm. The observed TPA in ZnO/ZnS nanocomposites is an instantaneous nonlinear process and is greatly enhanced compared to that in ZnS, ZnSe, and CdS QDs[11-13], which demonstrates that ZnO-based nanocomposites might be a promising candidate for photonic device applications at room temperature.

2 Experiments

The preparation procedures of ZnO/ZnS/Ag nanocomposite QDs are briefly described as follows. Zinc acetate and sodium hydroxide were dissolved in methyl alcohol, respectively, and stirred by magnetic stirrers. The two solutions were homogeneously mixed and the resulting reaction mixture was grown at 90 ℃ for 6 h. After centrifuged with distilled water and ethanol several times to remove the impurities, the precipitates were dried under vacuum at 60 ℃. The as-prepared ZnO/ZnS and ZnO/ZnS/Ag QDs were obtained with a similar procedure except that thioacetamide and silver nitrate were added into the solution respectively. Four ZnO-based nanocomposite samples have been investigated in this work. In Sample 1 and Sample 2, the ZnO/ZnS and ZnO/ZnS/Ag core/shell QDs were separately dissolved into the dimethy formamide (DMF) solvent and both concentrations are 0.1 g/L. For Sample 3 and Sample 4, ZnO/ZnS and ZnO/ZnS/Ag core/shell QDs were deposited on sapphire substrates to prepare for thin films with spin-coating technique. The morphology and size distribution of ZnO/ZnS and ZnO/ZnS/Ag core/shell QDs were inspected with a field emission scanning electron microscope (SEM) (Hitachi, S-4800) and a field emission high-resolution transmission electron microscope (HRTEM) (JEOL, JEM-2100F). The one-photon absorption spectra of the samples were recorded on a UV-visible spectrophotometer (Shimadzu, U-2800) in the range from 200 to 1 000 nm. The PL spectra of the samples were measured by a fluorescence spectrophotometer (Perkin-Elmer, LS-55) using a 450 W monochromatized xenon lamp with excitation wavelength of 295 nm.

3 Results and Discussion

SEM and HRTEM images as well as electron diffraction patterns of the ZnO-based nanocomposite core/shell QDs are shown in Fig. 1. The SEM pictures indicate that the clustered ZnO/ZnS/Ag QDs are beaded with some bright nano-dots, which is obviously different from ZnO/ZnS QDs. The HRTEM images clearly reveal that the ZnO/ZnS core/shell QDs are crystalline with an average diameter of ~9 nm. The obtained energy dispersive X-ray (EDX) spectroscopy and TEM electron diffraction patterns also confirm the ZnO/ZnS and ZnO/ZnS/Ag core/shell structures. The TEM electron diffraction pattern was matched against a simulated diffraction pattern generated using TEM simulator Java electron microscopy simulation (JEMS) software. With the experimental and the simulated diffraction patterns, it can be deduced that the ZnO/ZnS/Ag core/shell nanoparticles consist of ZnO core and ZnS shell with

hexagonal structure as well as Ag nano-dots with cubic structure. The TEM results are in good agreement with that of XRD, as shown in Fig. 2.

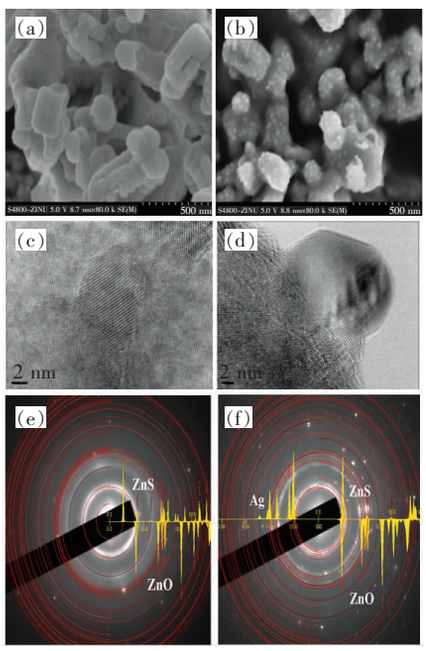

Fig. 1　SEM micrographs, HRTEM images and electron diffraction patterns of ZnO/ZnS (a), (c), (e) and ZnO/ZnS/Ag (b), (d), (f) nanocomposite QDs.

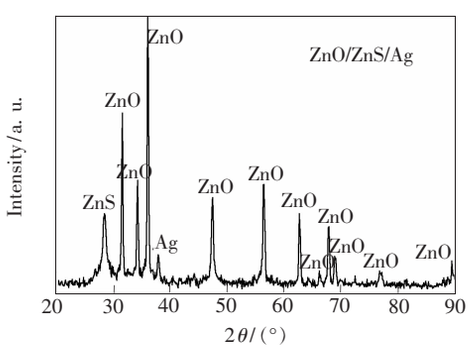

Fig. 2　XRD pattern of ZnO/ZnS/Ag nanocomposite QDs

The one-photon absorption spectra of the ZnO/ZnS and ZnO/ZnS/Ag core/shell QDs in DMF solution are shown in Fig. 3(a). The lowest excitonic transition is located at ~350 nm and the size of ZnO QDs is estimated to be ~ 5 nm[20], which is consistent with the TEM measurement. Broadening of the excitonic transition is primarily due to the inhomogeneity arising from size dispersion. Fig. 3(b) displays the PL spectra for the ZnO/ZnS and ZnO/ZnS/Ag core/shell QDs. The pure ZnO QDs were also characterized for comparison. The PL emission peak (~ 375 nm) is red-shifted compared to the excitonic transition (~ 350 nm) due to the Stokes shift. The PL intensity of ZnO/ZnS core/shell QDs is greatly enhanced compared to that of pure ZnO QDs while largely decreased as beaded with Ag nano-dots. The strong emission band (450 ~ 650 nm) in pure ZnO QDs could be attributed to the carrier recombination of the surface defect states, which are mostly suppressed in core/shell QDs due to the surface passivation.

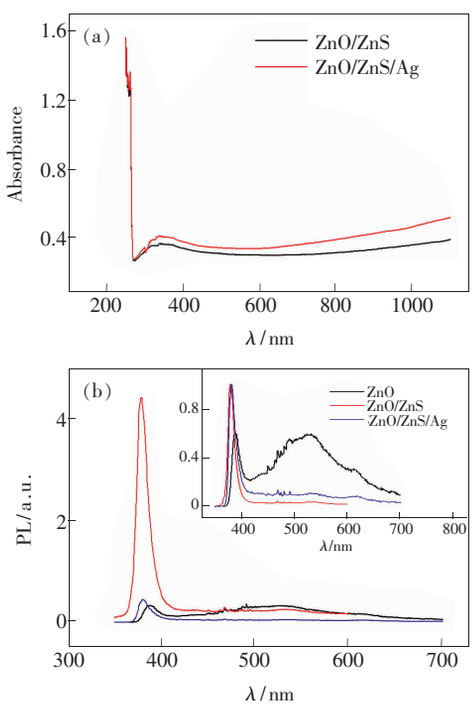

Fig. 3　UV-visible absorption spectra (a) and PL spectra (b) measured with excitation wavelength of 295 nm for ZnO/ZnS and ZnO/ZnS/Ag nanocomposite QDs. The inset shows the normalized PL spectra for comparison.

The room-temperature TPA of ZnO-based nanocomposites was investigated at the wavelength of 660 nm with a standard Z-scan technique[21]. The femtosecond laser pulse was produced by an optical parametric amplifier (TOPAS, USF-UV2), which was pumped by a Ti: Sapphire regenerative amplifier system (Spectra-Physics, Spitfire ACE-35F-2KXP, Maitai SP and Empower 30). The pulse repetition rate is 2 kHz and the minimum beam waist is about 40 μm. For comparison, similar TPA measurements were conducted on a 1.0 mm-thick hexagonal ZnO bulk crystal with laser polarization perpendicular to

its 〈0001〉 axis. Pure DMF solvent was examined under the same conditions and the nonlinear response was insignificant. All the Z-scans reported here were performed with excitation irradiances below the damage threshold.

Fig. 4(a) and 4(b) illustrate the open-aperture (OA) Z-scan curves for the ZnO/ZnS and ZnO/ZnS/Ag core/shell QDs in DMF solvent at different excitation irradiances (I_{00}), where I_{00} is denoted as the peak, on-axis irradiance at the focal point ($z=0$) within the sample. I_{00} is related to the incident irradiance by taking Fresnel's surface reflection into consideration. Based on a spatially and temporally Gaussian pulse, the normalized energy transmittance, $T_{OA}(z)$, is given by[22]

$$T_{OA}(z) = \frac{1}{\sqrt{\pi}q_0}\int_{-\infty}^{\infty}\ln[1+q_0\exp(-x^2)]\,dx, \quad (1)$$

where $q_0=\beta_2 I_0 L_{eff}$, β_2 is TPA coefficient, $L_{eff}=[1-\exp(-\alpha l)]/\alpha$, α is linear absorption coefficient, and l is the sample path length. The TPA coefficient β_2 can be extracted by fitting the above equation to the OA Z-scan curves. Fig. 4(a) and 4(b) indicate that theoretically fitting curves (solid lines) match well with the experimental data (symbols). The intrinsic TPA coefficient (β_{2QD}) and TPA cross section (σ_2) have been evaluated and summarized in Table 1. It is known that the nonlinear absorption coefficients are related to the third-order imaginary susceptibilities by[22]

$$\beta_2 = 3\pi \mathrm{Im}\chi^{(3)}/(\lambda n_0^2 c\varepsilon_0), \quad (2)$$

where n_0 is the linear refractive index, λ is the laser wavelength, c is the speed of light in vacuum, and ε_0 is the dielectric constant in vacuum. Thus, the intrinsic third-order susceptibilities of ZnO/ZnS and ZnO/ZnS/Ag core/shell QDs can be obtained by the use of Eq. (2) with the relation of $\mathrm{Im}\chi^{(3)}=f_v|f|^4\mathrm{Im}\chi^{(3)}_{QD}$, where f_v is the volume fraction of nanocom posite QDs in the DMF solution and f is the local field correction that depends on the dielectric constant of DMF solvent and QDs. The intrinsic TPA coefficient of QDs (β_{2QD}) can be deduced as $\beta_{2QD}=\beta_{2solution}n^2_{0solution}/(n^2_{0QD}f_v|f|^4)$[13]. The β_{2QD} obtained for ZnO/ZnS core/shell QDs is ~960 cm/GW,

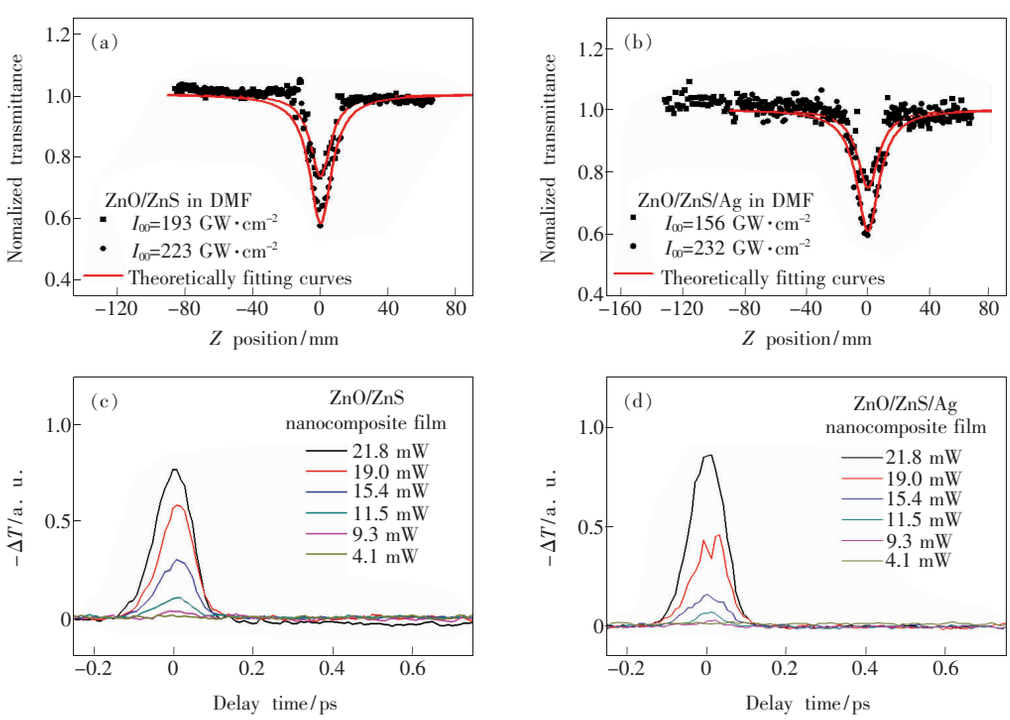

Fig. 4 Open-aperture Z-scans for ZnO/ZnS (a) and ZnO/ZnS/Ag (b) core/shell QDs in DMF solution at 660 nm at different excitation irradiances. The symbols denote the experimental data while the solid lines are the theoretically fitting curves. Degenerate, transient transmission measurements on ZnO/ZnS (c) and ZnO/ZnS/Ag (d) nanocomposite films at 660 nm.

which is ~1 000 times larger than that of the bulk ZnO and ZnS[16]. This enhancement can be attributed to the quantum confinement and optical Stark effects[1] since the average radius of ZnO core (~2.5 nm) is comparable to the Bohr exciton radius (~1.8 nm). We can convert the TPA coefficient (β_2) into the TPA cross-section (σ_2) by the definition of $\sigma_2 = \frac{\beta_2 h\nu}{N_0}$, where $h\nu$ is the photon energy, and N_0 is the density of nanocomposite QDs in the solution. By the use of calculated $N_0 = 6.2 \times 10^{13}$ cm^{-3}, the TPA cross-section of ZnO/ZnS core/shell QDs is found to be 4.3×10^{-44} cm^4 · s/photon = 4.3×10^6 GM, which is at least two orders of magnitude higher than that of ZnS, ZnSe, CdS QDs[11-13]. As presented in Table 1, the TPA in ZnO/ZnS core/shell QDs is improved as beaded with Ag nano-dots, which is attributable to local field enhancement[22-23]. The obtained TPA coefficient is intensity independent, which manifests a third-order nonlinear process. The TPA saturation or TPA-excited free carrier absorption is insignificant under the current experimental conditions[23-24]. In addition, we also determine the TPA and three-photon absorption (3PA) coefficients of the ZnO-based core-shell QDs unambiguously with the use of a Z-scan theory developed for materials that possess TPA and 3PA simultaneously[25]. Details of the calculation are not presented here but it verifies again that the TPA is dominant in the ZnO-based nanocomposite QDs.

Table 1　Crystallite size, one-photon absorption, intrinsic TPA, and TPA cross section of nanocomposite QDs

	Size measured by TEM/nm	Size estimated by XRD/nm	Lowest one-photon absorption transition/nm	TPA coefficient β_2/(cm · GW^{-1})	Intrinsic TPA coefficient β_{2QD}/(cm · GW^{-1})	TPA cross-section (σ_2)/(cm^4·s·photon^{-1})
ZnO/ZnS	9.0		350	0.008 9	9.6×10^2	~ 4.3×10^{-44}
ZnO/ZnS/Ag	9.0		350	0.009 4	1.0×10^3	~ 4.6×10^{-44}
ZnO QDs[14]	100 ~ 500		368	0.024		
ZnS QDs[12]		1.8	260	0.08		~ 1.7×10^{-46}
ZnSe/ZnS QDs[13]		4.5	410		2.17	~ 5.1×10^{-47}
ZnO (bulk)			375		1.3[21]	
ZnS (bulk)			337		0.35[16]	~ 5.1×10^{-52}[12]

In the pump-probe experiments, we employed a cross-polarized, pump-probe configuration[20] with 660-nm, 35-fs laser pulses from the same laser system used for the Z-scans. The intensity ratio of the pump to the probe was kept at least 20∶1. With the cross-polarized configuration, any "coherent artifact" on the transient signal was eliminated. It has been examined that the probe beam alone could not influence any nonlinear effect in our experiments. Fig. 4(c) and (d) illustrate the degenerate transient transmission signals ($-\Delta T$) as a function of the delay time for ZnO/ZnS and ZnO/ZnS/Ag core/shell nanocomposite films, respectively. For the ZnO bulk crystal, the transient transmission signals are mainly dominated by the autocorrelation function of the pump and probe pulses, which reveal that the TPA plays a key role in the observed nonlinear absorption since TPA is an instantaneous nonlinear process. When the excitation pump irradiance is increased to ~ 40 GW/cm^2, there is a long absorption tail with a characteristic time of ~100 ps or longer. This slow recovery process can be attributed to the absorption of TPA-excited free carriers in the bulk ZnO since the amplitude of the absorption tail grows proportionally to the square of the excitation pump irradiance (not shown in Fig. 4)[21]. However, the slow recovery processes do not manifest themselves in the ZnO-based nanocomposite films with the excitation irradiance up to ~300 GW/cm^2, which is the photo-induced damage threshold. The magnitude of main peaks in the measured dynamics increases proportionally with the excitation power,

which confirms that TPA is dominant.

4 Conclusion

In summary, the TPA coefficients of ZnO/ZnS and ZnO/ZnS/Ag core/shell QDs have been measured using femtosecond Z-scan and pump-probe techniques, and compared to that of bulk ZnO. The TPA cross-sections of ZnO-based core-shell nanocomposites are compared favorably to that of ZnS, ZnSe and CdS QDs. All the above-discussed merits demonstrate that ZnO-based core-shell QDs are promising for multi-photon excitation imaging applications.

References:

[1] Alivisatos A P. Semiconductor clusters, nanocrystals, and quantum dots [J]. *Science*, 1996, 271(5251):933-937.

[2] He G S, Tan L S, Zheng Q D, *et al.* Multi-photon absorbing materials: Molecular designs, syntheses, characterizations, and applications [J]. *Chem. Rev.*, 2008, 108(4):1245-1330.

[3] Ray P C. Size and shape dependent second order nonlinear optical properties of nanomaterials and their application in biological and chemical sensing [J]. *Chem. Rev.*, 2010, 110:5332-5365.

[4] Gholami-Kaliji S, Saievar-Iranizad E, Dehghani Z, *et al.* Photoluminescent and nonlinear optical properties of aqueous synthesised $Cd_{0.6}Zn_{0.4}Te$ nanocrystals in different temperatures [J]. *Micro Nano Lett.*, 2012, 7(5):460-463.

[5] Smith A M, Nie S. Semiconductor nanocrystals: Structure, properties, and band gap engineering [J]. *Acc. Chem. Res.*, 2010, 43:190-200.

[6] Rinnert H, Jambois O, Vergnat M. Photoluminescence properties of size-controlled silicon nanocrystals at low temperatures [J]. *J. Appl. Phys.*, 2009, 106(2):023501-1-10.

[7] He J, Ji W, Ma G H, *et al.* Excitonic nonlinear absorption in CdS nanocrystals studied using Z-scan technique [J]. *Chin. J. Appl. Phys.*, 2004, 95(11):6381-6386.

[8] Zhu Y W, Elim H I, Foo Y L. Multiwalled carbon nanotubes beaded with ZnO nanoparticles for ultrafast nonlinear optical switching [J]. *Adv. Mater.*, 2006, 18:587-592.

[9] Xing G C, Ji W, Zheng Y, *et al.* Doped ZnSe/ZnS quantum dots [J]. *Opt. Express*, 2008, 16(8):5710-5715.

[10] Ahn C H, Mohanta S K, Lee N E, *et al.* Enhanced exciton-phonon interactions in photoluminescence of ZnO nanopencils [J]. *Appl. Phys. Lett.*, 2009, 94(26):261904-1-3.

[11] Chon J W M, Gu M, Bullen C, *et al.* Three-photon excited band edge and trap emission of CdS semiconductor nanocrystals [J]. *Appl. Phys. Lett.*, 2004, 84:4472-4474.

[12] Nikesh V V, Dharmadhikari A, Ono H, *et al.* Optical nonlinearity of monodispersed, capped ZnS quantum particles [J]. *Appl. Phys. Lett.*, 2004, 84:4602-4604.

[13] Lad A D, Kiran P P, More D, *et al.* Two-photon absorption in ZnSe and ZnSe/ZnS core/shell quantum structures [J]. *Appl. Phys. Lett.*, 2008, 92(4):043126-1-3.

[14] Karthikeyan B, Suchand Sandeep C, Pandiyarajan S T, *et al.* Optical and nonlinear absorption properties of Na doped ZnO nanoparticle dispersions [J]. *Appl. Phys. Lett.*, 2009, 95(2):023118-1-3.

[15] He J, Ji W, Mi J, *et al.* Three-photon absorption in water-soluble ZnS nanocrystals [J]. *Appl. Phys. Lett.*, 2006, 88(18):181114-1-3.

[16] He J, Scholes G D, Ang Y L, *et al.* Direct observation of three-photon resonance in water-soluble ZnS quantum dots [J]. *Appl. Phys. Lett.*, 2008, 92(13):131114-1-3.

[17] Liao Y, Yu X F, Qiu Y, *et al.* Nonlinear photoluminescence of ZnO/ZnS nanotetrapods [J]. *Chem. Phys. Lett.*, 2008, 465(4-6):272-274.

[18] Shuai X M, Shen W Z. A facile chemical conversion synthesis of ZnO/ZnS core/shell nanorodes and deverse metal sulfide nanotubes [J]. *J. Phys. Chem.* C, 2011, 115:6415-6422.

[19] Chaudhuri R G, Paria S. Gold-based core/shell and hollow nanoparticles [J]. *Chem. Rev.*, 2011, 112:2373-2379.

[20] Madler L, Stark W J, Pratsinis S E. Rapid synthesis of stable ZnO quantum dots [J]. *J. Appl. Phys.*, 2002, 92:6537-6540.

[21] He J, Qu Y L, Li H P, *et al.* Three-photon absorption in ZnO and ZnS crystals [J]. *Opt. Express*, 2005, 13(23):9235-

9247.

[22] Sutherland R L. *Handbook of Nonlinear Optics* [M]. 2nd ed. New York: Marcel Dekker, 2003.

[23] Ma G H, Sun W X, Tang S H, *et al*. Size and dielectric dependence of the third-order nonlinear optical response of Au nanocrystals embedded in matrices [J]. *Opt. Lett.*, 2002, 27(12):1043-1045.

[24] Gu B, Lou K, Wang H T, *et al*. Dynamics of two-photon-induced three-photon absorption in nanosecond, picosecond, and femtosecond regimes [J]. *Opt. Lett.*, 2010, 35:417-419.

[25] Gu B, Wang J, Chen J, *et al*. Z-scan theory for material with two- and three-photon absorption [J]. *Opt. Express*, 2005, 13(23):9230-9234.

刘姝妤(1989 -),女,湖南邵阳人,硕士研究生,主要从事超快激光光谱学的研究。
E-mail: 278251380@qq.com

何军(1974 -),男,湖南衡东人,教授,博士生导师,2004 年于新加坡国立大学获得博士学位,主要从事非线性光学、超快光子学等方面的研究。
E-mail: junhe@csu.edu.cn